





Supporting Information for Loss of Insulin Signaling in Astrocytes Exacerbates Alzheimer-like Phenotypes in 5xFAD Mouse Model

Wenqiang Chen¹, Qian Huang², Ekaterina Katie Lazdon³, Antonio Gomes¹, Marisa Wong², Emily Stephens^{1,5}, Tabitha Grace Royal^{3,4}, Dan Frenkel^{1,3,4,*}, Weikang Cai^{1,2,*}, C. Ronald Kahn^{1*}

¹Section of Integrative Physiology and Metabolism, Joslin Diabetes Center and Department of Medicine, Harvard Medical School, Boston, MA 02215, USA

²Department of Biomedical Sciences, College of Osteopathic Medicine, New York Institute of Technology, Old Westbury, New York, 11568, USA

³Department of Neurobiology, George S. Wise Faculty of Life Sciences, Tel Aviv University, Tel Aviv, 69978, Israel

⁴Sagol School of Neuroscience, Tel Aviv University, Tel Aviv, 69978, Israel

⁵School of Medicine, Texas Tech University Health Sciences Center, Lubbock, Texas, 79430, USA

* C. Ronald Kahn; Weikang Cai; Dan Frenkel

Email: c.ronald.kahn@joslin.harvard.edu (C.R. Kahn); dfrenkel@tauex.tau.ac.il (D. Frenkel); wcai04@nyit.edu (W. Cai)

Lead contact: c.ronald.kahn@joslin.harvard.edu (C.R. Kahn)

This PDF file includes:

Supplementary Materials and Methods
Legends for Figures S1 to S7
Tables S1
Legends for Movies S1 to S2

Other supporting materials for this manuscript include the following:

Movies S1 to S2

Materials and Methods

Experimental animals

Mice expressing tamoxifen-inducible Cre recombinase (Cre^{ERT2}) in cells expressing GFAP (*GFAP^{CreERT2}*) were crossed with IR^{ff} mice to create iGIRKO mice (inducible astrocyte-specific IRKO mice), as previously described (16). iGIRKO mice and 5xFAD mice were crossed to create iGIRKO/5xFAD mice. For all the experiments, IR^{ff}, iGIRKO, 5xFAD, and iGIRKO/5xFAD littermates were generated from iGIRKO/5xFAD and IR^{ff} breeding pairs. All experimental mice with 5xFAD background were hemizygous for the *APP/PS1* transgene (21). Both male and female mice were included in behavioral and biochemical analyses unless otherwise specified in the figure legends.

Tamoxifen injection

Tamoxifen (T5648, Sigma-Aldrich) was prepared at a final concentration of 20 mg/mL in 10% ethanol and 90% peanut oil (P2144, Sigma-Aldrich). Six-week-old IR^{ff}, iGIRKO, 5xFAD, iGIRKO/5xFAD mice were injected i.p. with tamoxifen daily at a dose of 100 mg/kg for 5 consecutive days. Mice were subjected to various analysis at other time points as indicated. To ensure efficient IR KO in any newly generated astrocytes from neural progenitor cells along the progression of β -amyloid pathology, a second round of tamoxifen injection for 5 consecutive days was performed at the age of 3 months.

Vena cava insulin injection

Mice were fasted overnight (16 h) prior to the vena cava insulin injection (5 U per mouse). 15 min following insulin injection, mice were perfused with ice-cold PBS. Brain tissues were snap frozen in liquid nitrogen and stored in -80 °C until further biochemical and molecular analysis.

Blood Glucose and Plasma Insulin Determination

To measure fasting blood glucose levels, a small cut was made on the distal end of the tail using a sterile surgical blade. Approximately 2 μ L of venous blood was collected, and blood glucose concentration was measured using a glucometer (Bayer, Germany). For mice subjected to 4-hr fasting, food was withdrawn, and blood samples collected 4 hr later. To measure insulin levels, approximately 20 μ L of venous blood was collected as above, centrifuged for plasma collection, and insulin levels measured using an ultra-sensitive mouse insulin ELISA kit (90080, Crystal Chem, IL, USA).

Primary culture of mouse astrocytes

Isolation and culture of mouse primary astrocytes followed our previously reported protocol (16). Briefly, astrocytes were isolated from postnatal day 1 (P1) IR^{ff} mouse pups. Following removal of the brain, meninges were removed, and the prefrontal cortices were minced in ice-cold Hibernate A medium (A1247501, Gibco). The cortical tissues were then digested using Neural Tissue Dissociation Kit (P) (#130-092-628, Miltenyi Biotec) for 30 min at 37°C. Primary astrocytes were isolated using MACS anti-ACSA-2 microBeads (#130-097-678, Miltenyi Biotec) following the manufacturer's instruction. Isolated IR^{ff} or IGF1R^{ff} astrocytes were cultured on poly-D lysine-coated cell culture dishes in DMEM/F12 culture medium (#10565018, Gibco) supplemented with 10% FBS, 100 U/mL penicillin and 100 µg/mL streptomycin (#15140122, ThermoFisher), which was replaced every 3 days thereafter until the cell monolayer reached confluence. To induce IR and IGF1R deletion, IR KO astrocytes were obtained by infecting primary astrocytes with ad-CMV-iCre adenovirus (1x10⁷ PFU/mL, Vectorbiolabs) for 24 hrs and culturing for an additional 5 days before the experiments. Control cells were obtained using ad-CMV-luciferase adenovirus infection (1x10⁷ PFU/mL, Vectorbiolabs) in the same experimental duration.

Uptake of A β in primary mouse astrocytes

IRKO, IGF1RKO and their corresponding controls were serum-starved in DMEM/F12 with 0.1% BSA for 4 hr then stimulated with 100 nM insulin for 30 min. Following stimulation, cells were incubated with 0.1 mM A β ₁₋₄₂ HiLyte Fluor647 (AS-60480-01, Anaspec) and 100 nM insulin for either 1 or 24 hr followed by two washes with 1xPBS. Cells were detached from the cell culture plate using Accutase (A1110501, Gibco) and resuspended in FACS buffer (1% FBS + 0.25 mM EDTA) for flow cytometry analysis. Accuri C6 cytometer (BD biosciences) was used to gate the single cells and quantify the fluorescent intensity from HiLyte Fluor647-labeled A β ₁₋₄₂ for individual cells. The mean fluorescent intensity of each sample was calculated.

In situ A β update assay in brain slices

Knockout of IR in primary astrocytes in adult IR^{ff} mice was performed similar to the above-described method, except using adult animals. After reaching confluence, isolated astrocytes with or without IR KO were incubated with 100-µm brain slices prepared from 9-month-old 5xFAD mouse brain for 3 days in a tissue culture incubator at 37°C. In control experiment, brain slices were incubated with basal medium containing no astrocytes. 3 days after incubation, anti- β amyloid staining was performed to visualize A β size and areas on the brain slides. Image J software was used to analyze the size and areas of the A β plaques.

Seahorse analyses of mitochondrial stress and glycolytic stress

Seahorse XF24 analyses of mitochondrial and glycolytic stress in primary astrocytes were performed following the manufacturer's instructions. Briefly, 10,000 cells were seeded in an XF 24-well plate in 100 μ L growth media. One hour later, another 150 μ L of growth media was added to a final volume of 250 μ L. Plates were incubated in a tissue culture incubator overnight at 37 °C. In addition, a sensor cartridge was prepared by adding 1 mL of Seahorse Bioscience XF24 Calibrant (pH 7.4) to each well and incubated at 37 °C without CO₂ overnight. The next day, growth media was removed, and the cells were washed once with pre-warmed XF assay media. For the mitochondrial stress test, plates were incubated in 37 °C without CO₂ for 1 hr and the following compounds were loaded in the well in respective ports: oligomycin (2 μ M), FCCP (2 μ M), rotenone (2.5 μ M). For the glycolytic stress test, plates were incubated in 37 °C without CO₂ for 1 hr, and the following compounds were loaded in the well in respective ports: glucose (10 mM), oligomycin (2 μ M), 2-DG (50 mM). Results were normalized to protein content.

Brain lysate preparation

For lysates preparation, brain hemispheres were homogenized on ice in 5 volumes (w/v) of 0.1% Triton X-100 in TBS buffer, supplemented with protease inhibitor cocktail (EDTA free, 100X in DMSO, B14002, Bimake, TX, USA) and phosphatase inhibitor cocktail (B15002, 100X, Bimake, TX, USA). After sonication, homogenates were centrifuged at 100,000g for 1 hr at 4°C. The resulting supernatants represented the soluble enriched fraction. The pellets were re-suspended in 1 mL 1x RIPA extraction buffer (20-188, Millipore, MO, USA) supplemented with protease and phosphatase inhibitor cocktails. After sonication, homogenates were centrifuged at 100,000g for 1 hr at 4°C. The resulting supernatants represented the membrane enriched and detergent-soluble fractions. The pellets were resuspended in 1 mL 5 M guanidine-HCl (AAJ6078622, Fisher Scientific, MA, USA) solution overnight at 4°C and centrifuged at 20,000g for 1 hr at 4°C. The resulting supernatants represented the insoluble fraction. Protein concentrations were determined using Pierce BCA Protein Assay Kit (23227, ThermoFisher, MA, USA) prior to biochemical analysis.

RNA Extraction and qPCR analysis

Total RNA was extracted from brain tissue using TRIzol reagent (15596018, ThermoFisher, MA, USA) according to the manufacturer's instruction. RNA concentration and quality were determined using the NanoDrop 2000 (Thermo Scientific, Germany). 0.5 μ g total RNA from each sample was reverse transcribed to cDNA using random oligos and a High-Capacity cDNA Reverse Transcription Kit (4368813, ThermoFisher, MA, USA) according to the manufacturer's instructions. The resultant cDNA libraries were diluted 25X in ultrapure water. 2 μ L of the diluted cDNA template was used in 20 μ L reaction mixture for the quantitative real time-PCR in duplicates using the SYBR Green GoTaq® qPCR Kit (A6002, Promega, WI, USA) in a CFX Connect™ System (Bio-Rad, CA). Results were analyzed using the CFX Connect™ System (Bio-Rad, München, Germany) Software

and the comparative CT method. All data are expressed as $2^{-\Delta\Delta CT}$ for the gene of interest normalized to the housekeeping gene *Tbp* and presented as fold-change relative to controls. Sequences for each primer are listed in Supplementary Table 1.

Western blotting analysis

Western blotting analysis was performed according using our previously published protocols (2, 4). Total protein was extracted from snap-frozen tissues in ice-cold RIPA lysis buffer (20-188, Millipore, MO, USA) supplemented with 0.1 % SDS and 1x protease and phosphatase inhibitors cocktail (Bimake, TX, USA). 10 to 15 mg total protein extracts were loaded on NuPage 4-12% polyacrylamide gels (NP0321, ThermoFisher, MA, USA), and proteins were separated by electrophoresis. Proteins were transferred onto PVDF membranes (88518, ThermoFisher, MA, USA) for 3 hr at 90V in a cold room. Following transfer, membranes were blocked in StartingBlock buffer (37539, ThermoFisher, MA, USA) for 1 hr at room temperature, then PVDF membranes were incubated with the indicated primary antibodies overnight at 4 °C. The primary antibodies included rabbit anti-GAPDH (1:2000, #5174), rabbit anti-phospho-IR/IGF1R (1:1000, #3024), rabbit anti-p-Akt (1:1000, #9271), rabbit anti-Akt (1:1000, #4685), rabbit anti-p-ERK1/2 (1:1000, #9101; T202/Y204), rabbit anti-ERK1/2 (1:1000, #9102), rabbit anti-Beclin-1 (1:1000, #3495), rabbit anti-LC3B (1:1000, #2775), rabbit anti-p62 (1:1000, #5114), rabbit anti-PINK (1:1000, #6946) antibodies were all purchased from Cell Signaling Technologies. Rabbit anti-p-Tau (T231, 1:500, ab151559), rabbit anti-p-Tau (T212/S214, 1:500, ab4842), mouse anti-Tau (total, 1:1000, ab80579), mouse anti-BNIP3 (1:1000, ab10433) and rabbit anti-PSD95 (1:1000, #ab18258) antibodies were purchased from Abcam. Rabbit anti-p-IRS-1 (1:1000, #09-432; Y612) antibody was purchased from Millipore. Mouse anti-IRS-1 (1:1000, #611394) antibody was purchased from BD Biosciences. Rabbit anti-IR β (1:1000, #sc-711), mouse anti-phospho-IR β (1:200, #sc-81500), rabbit anti p-Tau (1:1000, S396, sc-12414-R) antibodies were purchased from Santa Cruz. After incubation with primary antibodies, membranes were washed 3 times with 1x PBS supplemented with 0.1% Tween-20 (PBST) and incubated with appropriate secondary antibodies conjugated to horseradish peroxidase (HRP) (1:10,000, Cell Signaling, MA, USA). Membranes were visualized with SuperSignal West Pico substrate (Pierce Biotechnologies, Rockford, IL) or Immobilon Western HRP Substrate (Millipore, Billerica, MA). Chemiluminescent signals were detected using X-ray films, and quantitation was performed using Image J software.

Mouse brain clearing, staining, and imaging

For enhanced volumetric (3D) immunofluorescent PVS imaging, two mice were processed. The anesthetized animals were transcardially perfused with 20 mL of ice-cold heparinized 1x PBS (20 U/mL heparin, 375095, Millipore-Sigma, MA, USA) until the fluid ran clear, followed by 20 mL of ice-cold 4% PFA (15714, Electron Microscopy Sciences, PA, USA). After perfusion, the right

hemispheres of the brains were collected and transferred to 1x PBS with 0.02% sodium azide at 4°C before shipping to LifeCanvas Technologies (MA, USA) for subsequent sample processing and imaging. Briefly, extracted brains were post-fixed and cleared for 5 days in SmartClear II Pro (LifeCanvas Technologies, MA, USA) using a stochastic electrotransport method (6) for rapid nondestructive processing of large and dense samples. Cleared brains were immunolabeled in SmartLabel (LifeCanvas Technologies, MA, USA) for 24 hrs using the following primary antibodies that against GFAP (644702, BioLegend, CA, USA), β -amyloid (8243S, Cell Signaling Technology, MA, USA) and Lectin DyLight™488 (DL-1174-1, Vector Laboratories, CA, USA). Fluorescently conjugated secondary antibodies against appropriate species were applied. Optimized refractive index matching was then performed by incubating immunolabelled brains in EasyIndex solution (LifeCanvas Technologies, MA, USA), a step that allows light to transpass tissue samples. A SmartSPIM light sheet microscope (LifeCanvas Technologies, MA, USA) was used to image the brains at 3.6x with a pixel size of 1.8 μm x 1.8 μm , axial resolution of about 4 μm , and Z-step size of 4 μm . A total of 1,650 sagittal images were generated for each mouse brain hemisphere. 3D image datasets from light sheet microscope were analyzed in SmartAnalytics to generate heat maps of β -amyloid plaque density that was aligned to Allen Brain Atlas (version 3, 2015, accessible at <https://atlas.brain-map.org/>) (7).

Analysis of CLARITY brain images

For data analysis of images from cleared brain, only Channel 2 (561 nm, GFAP) and Channel 3 (642 nm, β -amyloid) were included. Montage images of β -amyloid were generated at an increment of 400 μm . To analyze β -amyloid plaque deposition in the cerebral cortex, four representative sagittal sections (each contains 20 images) encompassing all major cerebral cortical areas were analyzed. Appropriate and universal fluorescent threshold was applied to all images to identify positive staining, before the quantification of total plaque counts, total area, average size of the plaques, and percentage of area of plaque deposits using in ImageJ software. To analyze astrocyte processes surrounding β -amyloid plaque deposit, stacks of 100 images were z-projected, composited, and pseudocolored (GFAP as green and β -amyloid as red), followed by a colocalization analysis in Image J software. Representative brain regions including cerebral cortex, hippocampus, thalamus, and brainstem were processed and analyzed as four regions of interest.

To generate a heatmap of β -amyloid across all the brain regions in Allen Brain Atlas, voxel count of β -amyloid deposit in 5xFAD and iGIRKO/5xFAD mouse brains was normalized to the control groups (IR^{fl/fl}) to identify brain regions that showed the relative abundance of β -amyloid.

Immunohistochemistry staining

Brain tissues fixed in 4% paraformaldehyde overnight at 4°C. 24 hrs later, tissues were dehydrated in 30% sucrose in 1x PBS for another 48 hrs and cut at 40 µm thickness using cryostat. Primary antibodies that were used for immunohistochemistry staining were: Iba1 (1:1000, #019-19741, Wako, Japan), C1q (1:200, ab182451, Abcam, UK), β-amyloid (1:500, ab201060, Abcam, UK), Synaptophysin (1:500, ab32594, Abcam, UK), goat anti-rabbit IgG conjugated to Alexa Fluor 488 (1:500, ab11008, Abcam, UK). Sections were incubated with selected primary antibodies overnight at 4°C with gentle shaking, followed by incubation with secondary antibody at room temperature for 1 hr and coverslipped with DAPI for counterstaining. Slides were scanned and analyzed using Image J software.

Y maze test

To assess spatial recognition memory in mice, the Y maze was performed using a Plexiglas maze purchased from MazeEngineers (Boston, MA, USA) and a slightly modified protocol (8). The Y maze apparatus consisted of three arms (30 cm in length and 8 cm in width) which diverged at a 120° angle from each other, forming a Y shape. Each arm was equipped with a guillotine door that could be operated manually by the experimenter. The maze was located in a testing room that has visual objects that served as distal spatial cues. During the test, three arms were randomly designated as the start arm (where the mouse was released to explore and was always open), a novel arm (which was closed off during the 1st trial but open during the 2nd trial), and the third arm (always open). The Y maze test consisted of two trials, separated by an inter-trial interval of 2 min. During the 1st trial, mouse was placed in the start arm and allowed to explore the maze for 5 min, while the novel arm was blocked off. After a 2-min interval, the 2nd trial was conducted, during which all three arms were accessible. The position and movement of the testing mouse were recorded and analyzed by ANY-maze software. Data were expressed as total time spent in the novel arm during the 5-min period.

Nesting test

Nesting tests were conducted as previously reported (9). Briefly, mice were individually housed in new cages for 24 hrs. A compressed cotton square (5 × 5 cm) was provided to each cage at 16:30 PM, about two hours before the onset of the dark phase. 16 hrs later, nest construction was evaluated and scored using a 5-point scale Deacon system (10).

Contextual fear conditioning test (CFC)

The CFC test was used to study the capability of associating contextual information to aversive stimulus. Freezing, a fear-specific response, was exhibited as absence of movement except for breathing. The test was conducted in a standard operant system (MazeEngineers, Boston, MA)

consisting of an interior acrylic chamber (17 cm in length and width, 25 cm in height) enclosed by an isolation chamber (50 cm in width and height, 40 cm in depth) that was sound attenuating. The interior acrylic chamber was equipped with an electrifiable grid floor, a scrambled electric shock generator, and a sound generator. A camera was attached to a camera holder in the isolation chamber to capture video. The test was conducted on two consecutive days and consisted of 3 sessions: contextual training, contextual test, and altered contextual test. Mice were brought to a testing room for acclimation for 30 min before being placed in the shock chamber for training and testing. On Day 1, a 5-min and 4-sec contextual training session was conducted, consisting of 2-min acclimation, 2-sec foot electrical shock (0.5 mA), 2-min inter-trial interval (ITI), 2-sec foot electrical shock (0.5 mA), and 1-min to lights out. On Day 2, during a contextual test, each testing mouse was placed into the same chamber with the same context for 5 min without an electrical foot shock. Before contextual training and contextual testing, all chambers were cleaned with 70% ethanol. At least 3 hr after contextual test, the third, altered contextual session was conducted. In this session, mice were placed in a chamber with different context (i.e., a different wall color and different visual cues) for 5 min without an electric foot shock. During the altered contextual session, a different cleaning product (Windex) was used before the session to provide a different odor cue. The movement of the testing animals was recorded and analyzed using ANY-maze (Stoelting, IL, USA) and a customized template. Analysis setting was chosen as 1.5-sec minimal freezing time and a 0.01% activity detection level.

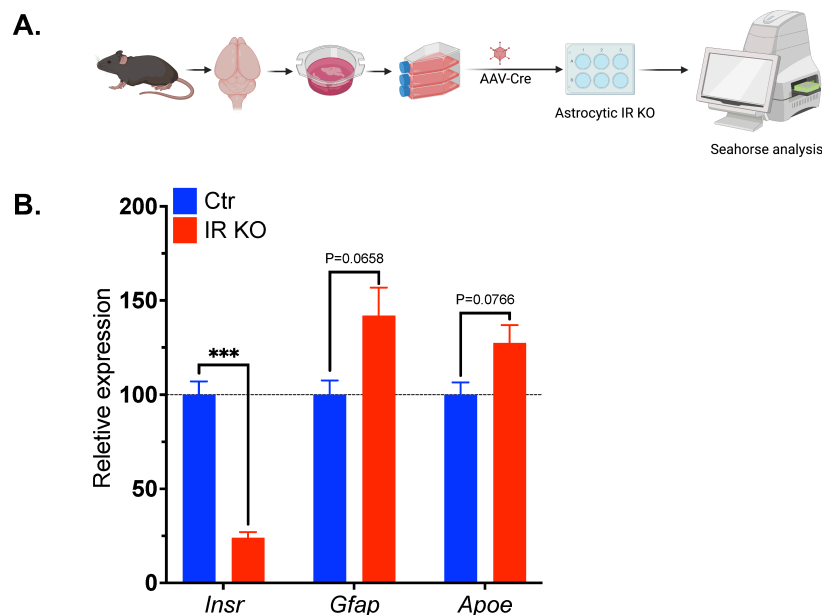


Figure S1. Loss of insulin signaling impairs mitochondrial respiration and glycolytic capacity in astrocytes (related to Figure 1).

(A) Schematic of Seahorse analysis of primary astrocytes with IR KO. **(B)** qPCR analysis showing the relative mRNA expression of *Insr*, *Gfap* and *Apoe* in control and IRKO astrocytes. *Tbp* was used as a control. ***, $P < 0.001$, unpaired t -test, $N = 3$. Data are presented as mean \pm SEM. Schematic was created with BioRender.

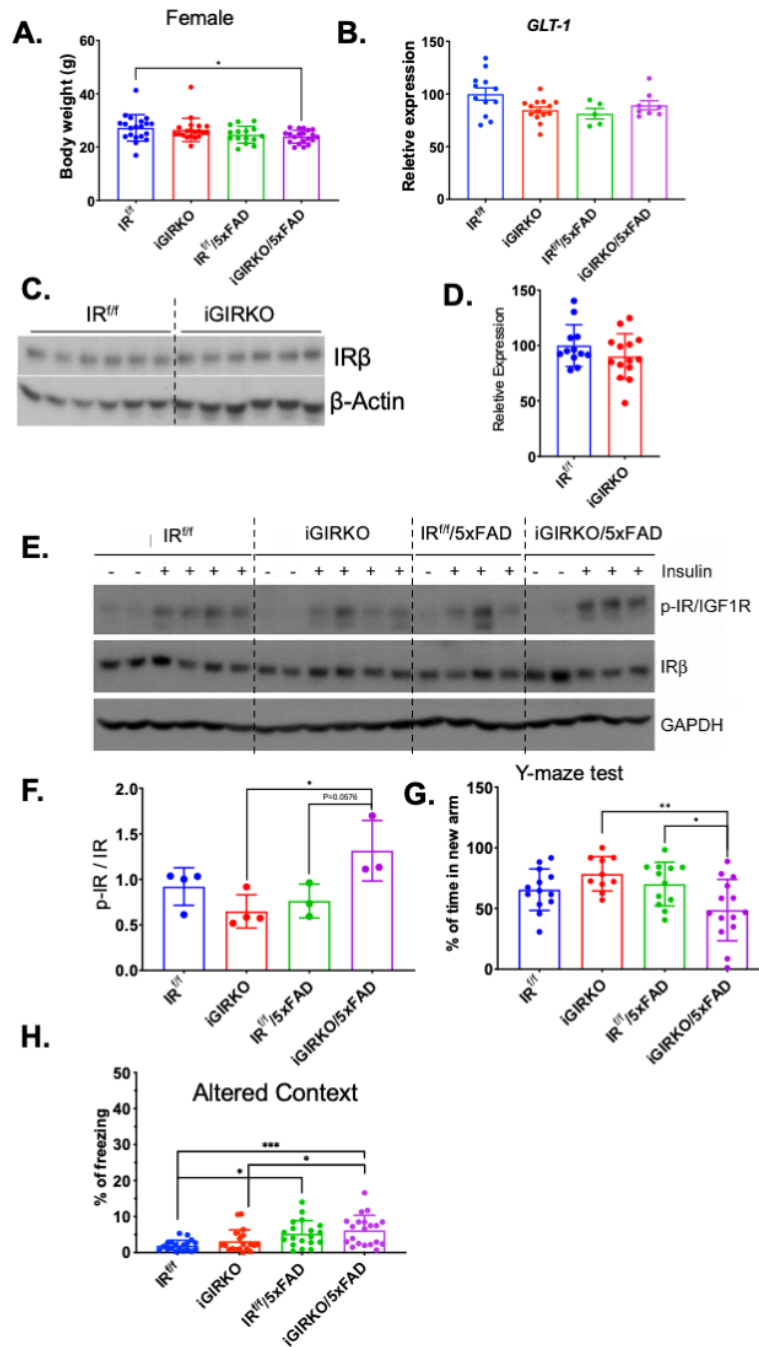


Figure S2. Establishment and characterization of 5xFAD mouse model with inducible IR KO in astrocyte (iGIRKO/5xFAD) (related to Figure 2).

(A) Measurement of body weight (g) at 6-month-old in female mice. N = 15 – 22 mice per condition. **(B)** qPCR analysis of astrocyte genes *Glt-1* in cortex of 8-month-old male mice. N = 5 – 14 mice per condition. **(C)** Representative western blots of insulin receptor β -subunit (IR β) in protein extracted from cortex of 8-month-old male mice. N = 4 – 6 per condition. **(D)** qPCR analysis of expression of *Insr* gene in the cortex of 8 month-old male mice. N = 5 – 14 per condition. **(E-F)** Representative western blots (E) and quantification (F) of phosphorylated β -subunit of IR/IGF1R in extracts from cortex of 6-month-old male mice. N=3 – 4 per condition. **(G)** Analysis of percent time of novel-arm exploration in the Y-maze in 6-month-old male mice (N = 10 – 14 mice per condition). **(H)** Percent of time with freezing behavior in conditioning test during the altered context test in 6-month-old male mice (N = 19 – 20 mice per condition). *, $P < 0.05$, ***, $P < 0.001$, by two-way ANOVA analysis followed by Tukey's multiple comparisons test. Quantitative data are presented as mean \pm SEM.

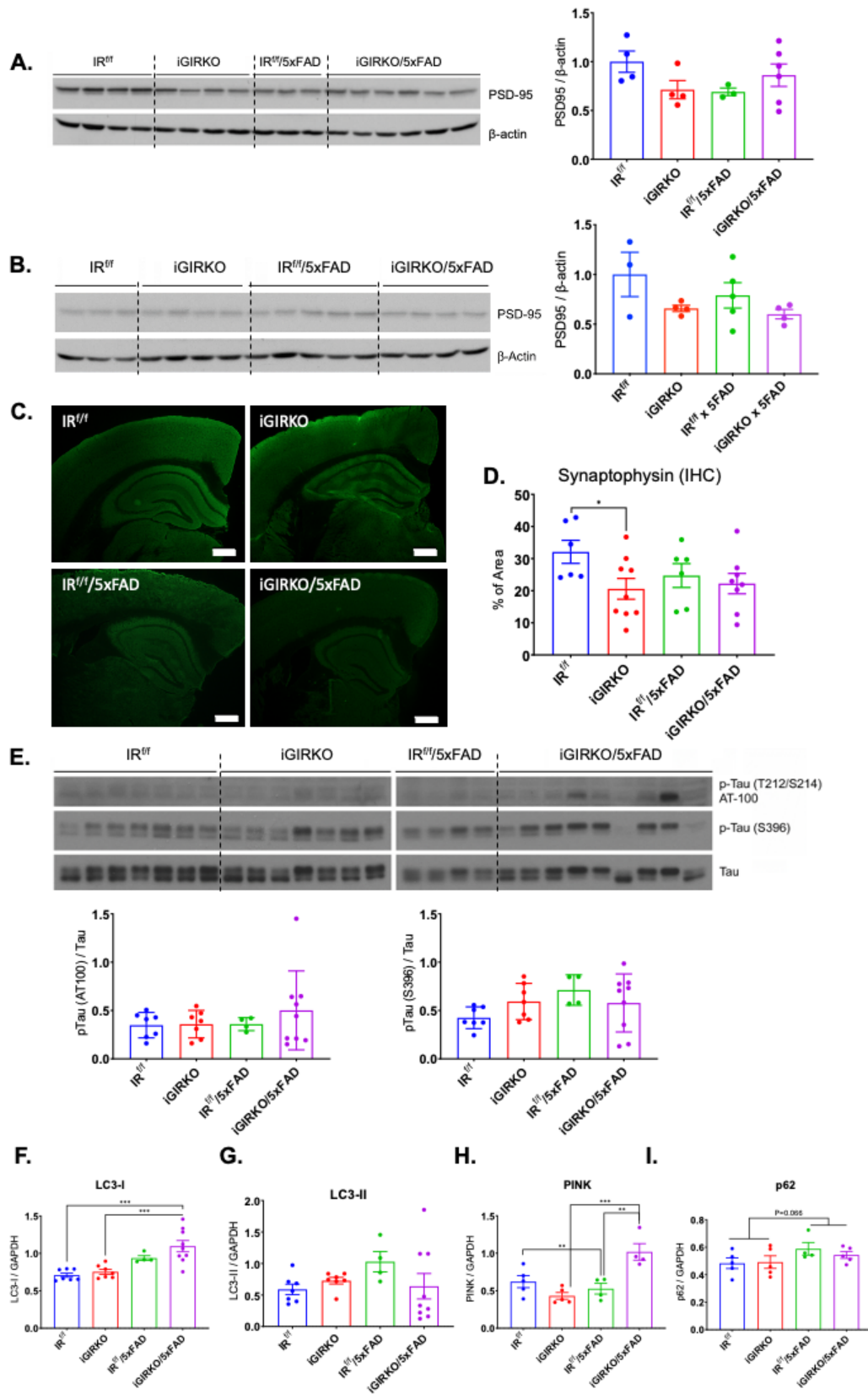


Figure 3S. Loss of insulin signaling in astrocytes enhances Tau phosphorylation, mitophagy, and autophagy (related to Figure 3).

(A-B) Representative western blot and quantification showing PSD95 protein levels in 8-month-old (A) male and (B) female mouse cortex. N = 3 – 6 per condition. **(C)** Representative images showing staining of synaptophysin proteins in the hippocampus of 7-month-old male. Scale bar: 500 μ m. **(D)** Statistical analysis of synaptophysin⁺ signals in the entire hippocampal region. Data are presented as mean \pm SEM. *, $P < 0.05$, student t-test. **(E)** Representative western blots and quantification of p-Tau (T212/S214 and S396) in protein extracted from cortex of 6-month-old male mice. N = 4 – 9 per condition. **(F-I)** Quantification of western blots (in Figure 3) of LC3-I (F), LC3-II (G), PINK (H), and p62 (I) in proteins extracted from cortex of 6-month-old male mice. N = 4 – 9 per condition. *, $P < 0.05$, **, $P < 0.01$, ***, $P < 0.001$ by two-way ANOVA analysis followed by Tukey's multiple comparisons test. Quantitative data are presented as mean \pm SEM.

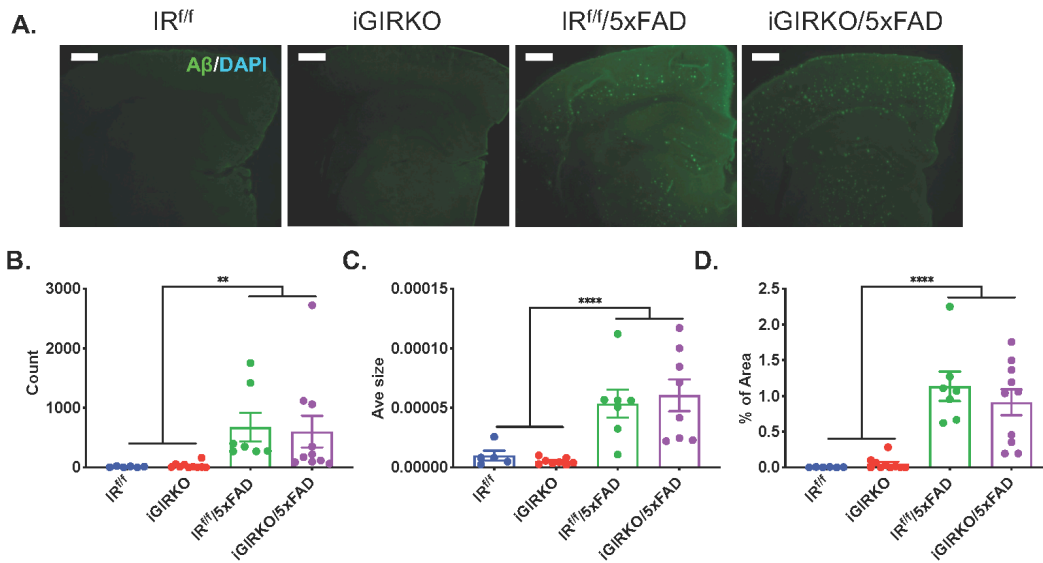


Figure 4S. Measurement of accumulation of A β plaque in the hippocampal CA1 and CA3 using immunohistochemistry staining (related to Figure 4).

(A) Representative images showing A β protein staining in the hippocampus of 7-month-old male. Scale bar: 100 μ m. **(B-D)** Statistical analysis of A β ⁺ signals in the hippocampal CA1 and CA3 regions normalized to the IR^{f/f} control mice, including count (B), Average size (C) and percentage of area (D). **, $P < 0.01$, ****, $P < 0.0001$ by two-way ANOVA analysis followed by Tukey's multiple comparisons test. Quantitative data are presented as mean \pm SEM.

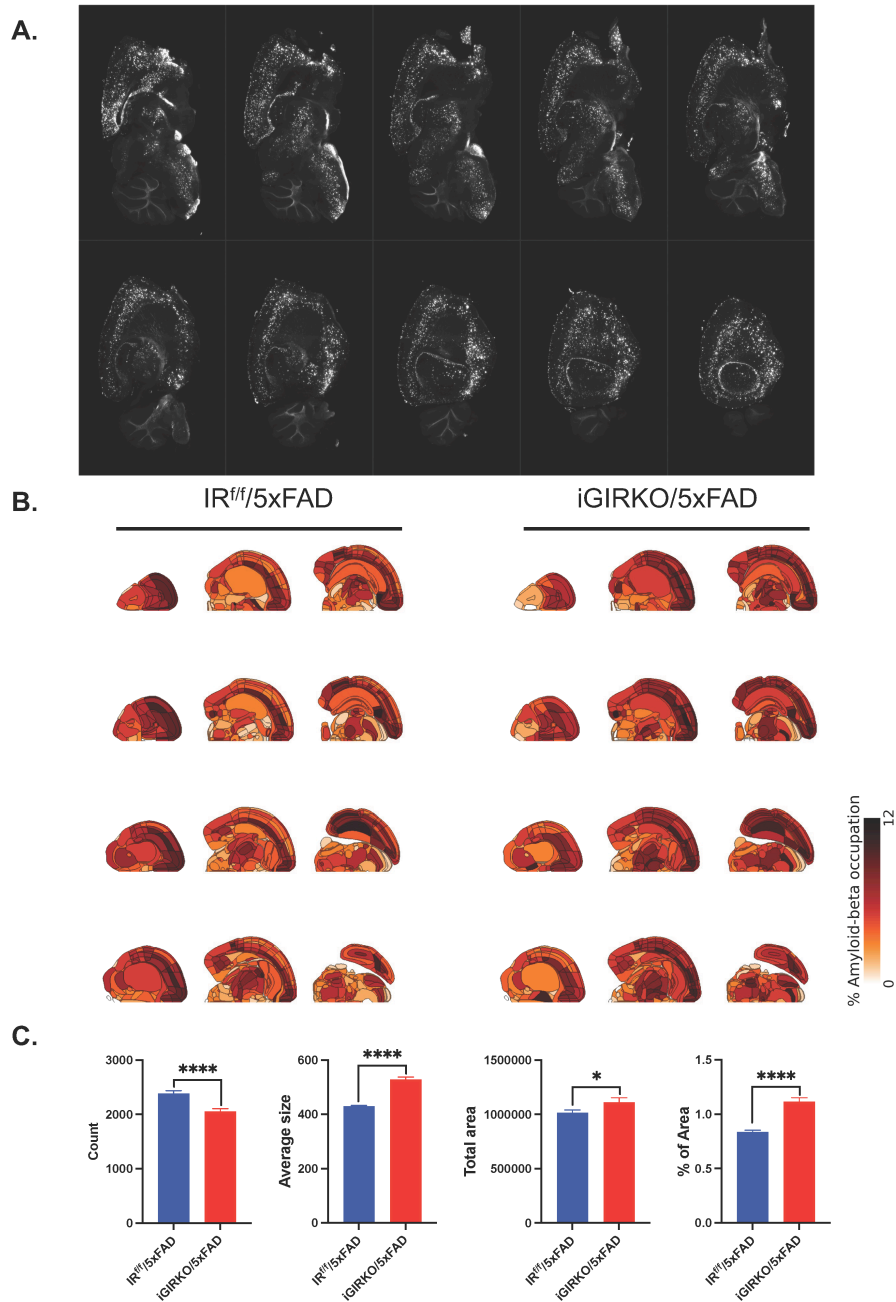


Figure 5S. Loss of astrocyte insulin signaling in mice leads to accumulation of A β plaque in the brain (related to Figure 4).

(A) Representative montage images showing A β plaque in the cerebral cortex of a male iGIRKO/5xFAD mice (increment = 400 μ m). **(B)** Representative density maps demonstrating A β plaque density in different brain regions. **(C)** Quantification of A β plaque in the whole brain of male IR^{fl/fl}/5xFAD and iGIRKO/5xFAD mice. N = 160 images from four mice were analyzed. *, $P < 0.05$, ****, $P < 0.0001$ by two-way ANOVA analysis followed by Tukey's multiple comparisons test. Quantitative data are presented as mean \pm SEM.

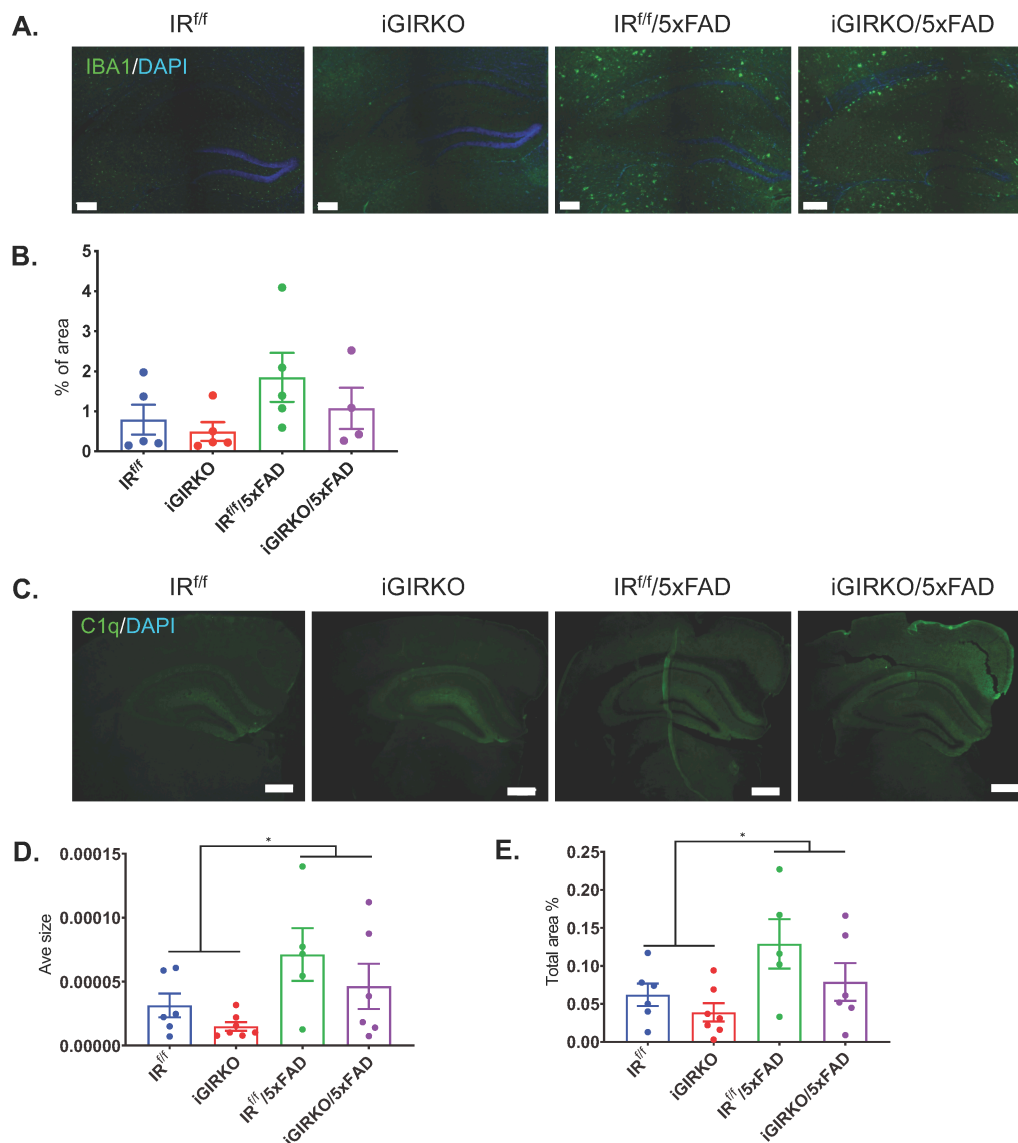


Figure 6S. Measurement of microglia activation in the hippocampus using immunohistochemistry staining (related to Figure 4).

(A) Representative images showing IBA1 protein staining in the hippocampus of 7-month-old male. Scale bar: 100 μ m. **(B)** Statistical analysis of IBA1⁺ signals in the hippocampal CA1 and CA3 regions. **(C)** Representative images showing C1q protein staining in the hippocampus of 7-month-old male. Scale bar: 100 μ m. **(D-E)** Statistical analysis of C1q⁺ signals in the entire hippocampal region, including Average size (D) and percent (%) of total area (E). *, $P < 0.05$, by two-way ANOVA analysis followed by Tukey's multiple comparisons test. Quantitative data are presented as mean \pm SEM.

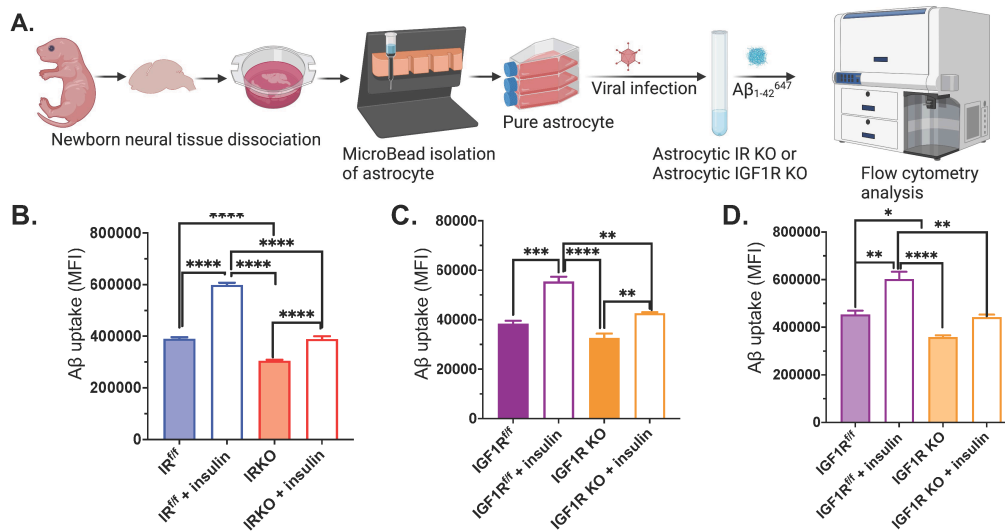


Figure 7S. Loss of insulin signaling in astrocyte impairs uptake of soluble neurotoxic Aβ₁₋₄₂ peptide (related to Figure 5).

(A) Schematic showing the workflow of analyzing Aβ₁₋₄₂ HiLyte Fluor647 labeled signals inside isolated astrocytes from neonatal pups. **(B)** Mean fluorescent intensity (MFI) analysis of HiLyte Fluor647 labeled Aβ₁₋₄₂ inside sorted P1 astrocytes (IR^{ff}) following 24-hr incubation. N = 5 – 6 per condition. **(C-D)** MFI analysis of HiLyte Fluor647 labeled Aβ₁₋₄₂ uptake inside sorted P1 astrocytes (IGF1R^{ff}) following 1-hr **(C)** or 24-hr **(D)** incubation. N = 3 per condition. *, *P* < 0.05, **, *P* < 0.01, ***, *P* < 0.001 by unpaired *t*-test. Data are presented as mean ± SEM. Schematic was created with BioRender.

Movie S1. 2D visualization of sagittal images (related to Figure 4)

Movie showing accelerated playing of sagittal images across a brain hemisphere. Movie was created using Image J.

Movies S2. 3D visualization of brain hemispheres (related to Figure 4).

3D movie showing a brain hemisphere cleared by LifeCanvas' SHIELD technology, with red fluorescent signals represent β-amyloid staining. Movie was created using Imaris.

Supplementary Table 1. Primers used for qPCR

Gene Symbol Primer direction Primer sequence

TBP Forward ACCCTTCACCAATGACTCCTATG
TBP Reverse TGACTGCAGCAAATCGCTTGG
IR Forward AAATGCAGGAACTCTCGGAAGCCT
IR Reverse ACCTTCGAGGATTTGGCAGACCTT
GFAP Forward GAAAACCGCATCACCATTCC
GFAP Reverse CTTAATGACCTCACCATCCCG
GLT-1 Forward TAACTCTGGCGGCAATGGAAAGT
GLT-1 Reverse ACGCTGGGGAGTTTATTCAAGAAT
ApoE Forward CAATTGCGAAGATGAAGGCTC
ApoE Reverse TAATCCCAGAAGCGGTTTCAG
SREBF2 Forward GCG TTC TGG AGA CCA TGG A
SREBF2 Reverse ACA AAG TTG CTC TGA AAA CAA ATC A
LRP1 Forward GCG ATG AGA GTG TCC GCA TA
LRP1 Reverse CGT GTG CCA GTT AGT CCA GT
GS Forward TGA ACA AAG GCA TCA AGC AAA TG
GS Reverse CAG TCC AGG GTA CGG GTC TT
Glut1 Forward GTGACGATCTGAGCTACGGG
Glut1 Reverse AACGGACGCGCTGTA ACTAT
MCT4 Forward CCTGTCATGCTTGTGGGTG
MCT4 Reverse GGAAGGCTGGAAGTTGAGAG
ASPA Forward ACA TGG CTG CTG TTA TTC ATC C
ASPA Reverse GGG TAC ACG GTA CAG TCT CCA
ICA1 Forward AGA GGG AAC AAG CGT TTT GTC
ICA1 Reverse TGG GTC CTG AGC ATG TGT CA
GAD2 Forward TCC GGC TTT TGG TCC TTC G
GAD2 Reverse ATG CCG CCC GTG AAC TTT T
NRF2_F. CTCGCTGGAAAAAGAAGTG
NRF2_R CCGTCCAGGAGTTCAGAGG
Dlg4 Forward TCT GTG CGA GAG GTA GCA GA
Dlg4 Reverse CGG ATG AAG ATG GCG ATA G
Syp Forward AGTGCCCTCAACATCGAAG
Syp Reverse GCCACGGTGACAAAGAATTC
Stx1a Forward ATTGGAAGACATGCTGGAGAG
Stx1a Reverse ACTGTGTCTGGTCTCGATCTC
mtND1 Forward TGC CAG CCT GAC CCA TAG CC
mtND1 Reverse ATG GGC CGG CTG GGT ATT CT
mtCytB Forward ACC AAT CTC CCA AAC CAT CA
mtCytB Reverse TCC AGA GAC TTG GGG ATC TAA C
mtATP6 Forward CAG TCC CCT CCC TAG GAC TT
mtATP6 Reverse TCA GAG CAT TGG CCA TAG AA

References

1. J. C. Bruning *et al.*, Role of brain insulin receptor in control of body weight and reproduction. *Science* **289**, 2122-2125 (2000).
2. W. Cai *et al.*, Insulin regulates astrocyte gliotransmission and modulates behavior. *J Clin Invest* **128**, 2914-2926 (2018).
3. H. Oakley *et al.*, Intraneuronal beta-amyloid aggregates, neurodegeneration, and neuron loss in transgenic mice with five familial Alzheimer's disease mutations: potential factors in amyloid plaque formation. *J Neurosci* **26**, 10129-10140 (2006).
4. K. Wardelmann *et al.*, Insulin action in the brain regulates mitochondrial stress responses and reduces diet-induced weight gain. *Mol Metab* **21**, 68-81 (2019).
5. Y. G. Park *et al.*, Protection of tissue physicochemical properties using polyfunctional crosslinkers. *Nat Biotechnol* 10.1038/nbt.4281 (2018).
6. S. Y. Kim *et al.*, Stochastic electrotransport selectively enhances the transport of highly electromobile molecules. *Proc Natl Acad Sci U S A* **112**, E6274-6283 (2015).
7. Q. Wang *et al.*, The Allen Mouse Brain Common Coordinate Framework: A 3D Reference Atlas. *Cell* **181**, 936-953 e920 (2020).
8. Y. Akwa, N. Ladurelle, D. F. Covey, E. E. Baulieu, The synthetic enantiomer of pregnenolone sulfate is very active on memory in rats and mice, even more so than its physiological neurosteroid counterpart: distinct mechanisms? *Proc Natl Acad Sci U S A* **98**, 14033-14037 (2001).
9. L. Devi, M. Ohno, TrkB reduction exacerbates Alzheimer's disease-like signaling aberrations and memory deficits without affecting beta-amyloidosis in 5XFAD mice. *Transl Psychiatry* **5**, e562 (2015).
10. R. M. Deacon, Assessing nest building in mice. *Nat Protoc* **1**, 1117-1119 (2006).